Geometrical and Electronic Structures of Gold, Silver, and Gold−Silver Binary Clusters: Origins of Ductility of Gold and Gold−Silver Alloy Formation

Han Myoung Lee, Maofa Ge, B. R. Sahu, P. Tarakeshwar, and Kwang S. Kim*

National Creative Research Initiative Center for Superfunctional Materials, Department of Chemistry, Division of Molecular and Life Sciences, Pohang University of Science and Technology, San 31, Hyojadong, Pohang 790-794, Korea

Received: March 31, 2003; In Final Form: June 10, 2003

The structures of pure gold and silver clusters (Au_k, Ag_k, $k = 1-13$) and neutral and anionic gold−silver binary clusters (Au_mAg_n, $2 \leq k = m + n \leq 7$) have been investigated by using density functional theory (DFT) with generalized gradient approximation (GGA) and high level ab initio calculations including coupled cluster theory with relativistic ab initio pseudopotentials. Pure Au_k clusters favor 2-D planar configurations, while pure Ag_k clusters favor 3-D structures. In the case of Au, the valence orbital energies of 5d are close to that of 6s. This allows the hybridization of 6s and 5d orbitals in favor of planar structures of Au_k clusters. Even 1-D linear structures show reasonable stability as local minima (or as global minima in a few small anionic clusters). This explains the ductility of gold. On the other hand, the Ag-4d orbital has a much lower energy than the 5s. This prevents hybridization, and so the coordination number (Nc) of Ag in Ag_k tends to be large in s-like spherical 3-D coordination in contrast to that of Au in Au_k which tends to be small in 1-D or 2-D coordination. This trend is critical in determining the cluster structures. The calculated electronic properties and dissociation energy of both pure and binary clusters are in good agreement with the available experimental data. Since the Ag-5s orbital is much higher in energy than the Au-6s orbital energy, the partial charge transfer from Au to Ag takes place in gold−silver binary clusters. Au atoms tend to be negatively charged, while Ag atoms tend to be positively charged. Combined with the trend that Au atoms favor the surface, edges, or vertices with smaller Nc, the outer part of the cluster tends to be negatively charged, while Ag atoms favor the inside with larger Nc, and so the inner part tends to be positively charged. The partial charge transfer in the binary system results in electrostatic energy gain for the binary Au_mAg_n cluster over pure Au_k and Ag_k clusters, which is responsible for the formation of alloys. In a neutral alloy, the equivalent mixing is favored, and the even numbered k tends to be more stable due to the electron spin pairing, whereas in an anionic alloy the odd numbered k tends to be more stable.

1. Introduction

The intense quest toward the design of novel nanofunctional materials (such as quantum dot, nanoclusters, and nanowires) has motivated several studies on small-sized metallic clusters (either with or without interaction with ligands).[1−4] The goal of most of these studies is to examine the modulation of the physical properties as a result of a decrease in the size. The dominance of quantum effects in such small dimensions leads to the emergence of several interesting characteristics. Bimetallic clusters, in particular, have drawn considerable attention in recent years due to their unique electronic, magnetic, optical, and mechanical properties. For example, a new class of highly efficient optical materials based on Au_mAg_n clusters (to be denoted as "*m*.*n*"), having vastly enhanced optical nonlinearity over the bulk metals, have recently been synthesized.[5,6] They are considered to be a promising class of catalysts that exhibit superior properties compared to pure metals, in terms of activity, selectivity, stability, and resistance to poisoning.[7] Gold−silver clusters and nanoparticles play an important role in catalysis, colloidal chemistry, and medical science.[8] New molecular nanocrystalline materials with gold and silver nanoclusters and nanowires, which would be considered as prototypes for electronic nanodevices and biosensors, have also been synthesized.[9]

Although much of the experimental and theoretical work so far has been done on pure gold and silver clusters and nanoparticles,[10−25] much less is known about the geometrical structures and energetics of binary clusters. These nanoclusters are expected to exhibit interesting electronic and spectral properties, which dramatically change with their sizes. On the experimental side, there are reports on the measurement of dissociation energy (D_0) of AuAg using resonant two-photon ionization spectroscopy.[13] An anion photoelectron spectroscopy (PES) study on Au_mAg_n ($2 \leq k = m + n \leq 4$) clusters is available only recently.[14]

In a while, the structures of gold and silver clusters have been theoretically investigated by a few research groups. Koutecky and co-workers[20] did a detailed study of structural isomers of small neutral and anionic silver clusters up to nonamer by using Hartree−Fock and correlated ab initio methods. Fournier[21] studied the silver clusters at the levels of DFT (VWN), sum of square-roots of atomic coordinations (SSAC), and extended Hückel molecular orbital (EHMO) theory. Gronbeck and Andreoni[22] used 11 e^- pseudopotential and studied the ground-state structures of gold clusters with Becke−Lee−Yang−Parr (BLYP) exchange-correlation functionals. Landman and co-

* Corresponding author phone: 82-54-279-2110; fax: 82-54-279-8137, 3399; e-mail: kim@postech.ac.kr.

10.1021/jp034826+ CCC: $25.00
Published on Web 08/26/2003

TABLE 1: Comparison of Calculated and Experimental Adiabatic Ionization Potentials (IP_a in eV), Vertical Detachment Energies (VDE in eV) [or Electron Affinities (EA in eV) in Brackets], Dissociation Energies (D_0 or $2D_0^*$ in eV), and Bond Lengths (r in Å in the Dimer) of Neutral and Anionic Au, Ag, Au_2, AuAg, and Ag_2[a]

		IPa			VDE [EA]			D_0 (neutral), D_0' (anion)			r		
Au_mAg_n	($m.n$)	BPW EC (SDB)	MP2 EC (SDB)	expt	BPW EC (SDB)	MP2 EC (SDB)	expt	BPW EC (SDB)	MP2 EC (SDB)	expt	BPW EC (SDB)	MP2 EC (SDB)	expt
Au	(1.0)	9.52(9.56)	8.39(9.23)	9.23	[2.17(2.25)]	[1.55(2.11)]	[2.31]						
Ag	(0.1)	7.91(8.04)	6.76(7.47)	7.57	[1.05(1.32)]	[0.55(1.00)]	[1.30]						
Au_2	(2.0)	9.32(9.38)	8.60(9.59)	9.20 ± 0.21	[1.88(1.88)]	[1.36(1.66)]	[1.94]	2.07(2.02)	1.99(2.44)	2.29 ± 0.008	2.55(2.54)	2.53(2.47)	2.47
AuAg	(1.1)	8.61(9.71)	7.62(8.64)	<9.15	[1.35(1.41)]	[0.86(1.10)]	[1.31]	1.98(2.02)	1.78(2.37)	2.08 ± 0.1	2.57(2.55)	2.58(2.49)	2.50
Ag_2	(0.2)	7.83(7.97)	6.68(7.60)	7.65	[0.96(1.04)]	[0.51(0.65)]	[1.02]	1.64(1.63)	1.26(1.81)	1.65 ± 0.03	2.58(2.57)	2.62(2.50)	2.48, 2.53
Au_2^-	(2.0)				2.01(2.00)	1.46(1.77)	2.01 ± 0.01	1.78(1.76)	1.80(1.99)	1.92 ± 0.15	2.67(2.66)	2.62(2.56)	2.58
$AuAg^-$	(1.1)				1.46(1.52)	0.97(1.20)	1.43 ± 0.08	1.17(1.19)	1.10(1.36)	1.08 ± 0.1	2.70(2.68)	2.71(2.59)	
Ag_2^-	(0.2)				1.02(1.13)	0.58(0.73)	1.06 ± 0.02	1.56(1.37)	1.22(1.46)	1.37 ± 0.16	2.69(2.70)	2.75(2.60)	2.60

[a] The experimental IP, VDE, and EA values are obtained from refs 12−14. The experimental D_0 and r values are taken from refs 12 and 13. The experimental Ag dimer distance is reported to be 2.53 Å (refs 12 and 15) and 2.48 Å (refs 12 and 16).

workers[23] used the Born−Oppenheimer local-spin density molecular dynamics (BO-LSD-MD) method with 11 e^- effective core potential (ECP) for small gold clusters. Ab initio calculations[25] of AuAg and Au_mAg_n anionic clusters are available only up to $k = 3$ (See Note Added in Proof.). Thus, there is a need for characterization of geometrical structures, electronic structures, and energetics of the clusters which is crucial for understanding various physical and chemical properties and stability of these clusters. Such a study would also aid the design of novel metallic nanostructures.

We thus present in this paper a systematic ab initio study of pure silver and gold clusters and gold−silver binary clusters at their neutral and anionic states. We find some interesting trends for the geometrical structures of binary clusters. The structures and energetics of pure silver and gold clusters up to $k = 13$ are reported. The agreement of the calculated vertical electron-detachment energies (VDE) with the available anion PES data[12] supports our geometrical assignments to these small anionic clusters. The vertical ionization potentials (IP_v) of neutral species are calculated and compared with the experimental data. The successive binding energies (sBE) of these binary clusters show odd−even oscillations, as in pure gold and silver clusters. In particular, the cluster formation in favor of binary alloys Au_m-Ag_n over pure Ag_k and Au_k clusters is investigated in terms of dissociation energy.

2. Calculation Methods

We used generalized gradient approximation (GGA) of Becke and Perdew[26] for exchange and correlation functional (BPW) and employed the relativistic ab initio 19-electron pseudopotentials for gold and silver from the Ermler-Christiansen (EC) family with the primitive basis set (5s5p4d).[27,28] We also performed calculations with the relativistic 19-electron Stuttgart−Dresden−Bonn (SDB) pseudopotentials[29] with the basis sets (8s7p6d2f)/[6s5p3d2f] developed by Martin recently.[30] The reliability of these calculation methods and basis sets was confirmed by the comparison of their results of the dimer systems with the experimental data. Here, we denote the BPW calculations with EC and SDB potentials as BPW/EC and BPW/SDB levels of theory. By using the same basis sets, the second-order Møller−Plesset perturbation method (MP2) calculations for the dimer systems were performed, and their results were compared with the BPW results. Additionally coupled cluster theory with singles and doubles excitations (CCSD) calculations were carried out on the MP2 optimized geometries using SDB pseudopotentials with [6s5p3d2f] basis sets to compare the relative stabilities of pure 1-, 2-, and 3-D gold and silver clusters. The Gaussian 98 and ACES codes[31] have been used for all the calculations. Most of the figures plotted here were drawn using the Pohang Sci-Tech Molecular Modeling (POSMOL) package.[32]

3. Results and Discussion

A. Dimeric Systems of Gold and Silver. We begin with the discussion of neutral and anionic Au_2, AgAu, and Ag_2 clusters (to be denoted as 2.0, 1.1, and 0.2). Table 1 shows the comparisons of their calculated and experimental adiabatic ionization potentials (IP_a), vertical detachment energies (VDE), electron affinities (EA), and dissociation energies with zero point energy (ZPE) correction (D_0). In the case of anionic dimers, D_0' is often used: $D_0'(AuAg^-) = D_0(AuAg) + EA(AuAg) - EA(Au)$; $D_0'(M_2^-) = D_0(M_2) + EA(M_2) - EA(M)$, where M = Au/Ag.

In the case of Au and Ag atoms, the experimental EAs are 2.3 and 1.3 eV;[14] the BPW/EC (and BPW/SDB) values are 2.2 (2.3) and 1.1 (1.3) eV; the MP2/EC (and MP2/SDB) values are 1.6 (2.1) and 0.6 (1.0) eV. The experimental IPs of Au and Ag are 9.2 and 7.6 eV;[12] the BPW/EC (and BPW/SDB) values are 9.5 (9.6) and 7.9 (8.0) eV; the MP2/EC (and MP2/SDB) values are 8.4 (9.2) and 6.8 (7.5) eV.

For Au_2, AuAg, and Ag_2, the experimental adiabatic IPs (IP_as) [9.2, <9.1, and 7.7 eV, respectively][12,13] are in good agreement with the BPW/EC (and BPW/SDB) values [9.3 (9.4), 8.6 (9.7), and 7.8 (8.0) eV] and in reasonable agreement with the MP2/EC (and MP2/SDB) values [8.6 (9.6), 7.6 (8.6), and 6.7 (7.6) eV]. The MP2/EC values are somewhat small. A similar trend is noted for D_0 (or $2D_0^*$ where D_0^* is the dissociation energy per atom), with the experimental values [2.3, 2.1, and 1.7 eV, respectively],[12,13] the BPW/EC (and BPW/SDB) values [2.1 (2.0), 2.0 (2.0), and 1.6 (1.6) eV], and the MP2/EC (and MP2/SDB) values [2.0 (2.4), 1.8 (2.4), and 1.3 (1.8) eV]. The experimental EAs [1.9, 1.3, and 1.0 eV, respectively][12,14] are also close to the BPW/EC (and BPW/SDB) values [1.9 (1.9), 1.3 (1.4), and 1.0 (1.0) eV], but the MP2/EC (and MP2/SDB) values [1.4 (1.7), 0.9 (1.1), and 0.5 (0.7) eV] are highly underestimated. A similar trend is also noted in the cases of Au_2^-, $AuAg^-$, and Ag_2^- for which the experimental VDEs [2.0, 1.4, and 1.1 eV, respectively][12,14] are similar to the BPW/EC (and BPW/SDB) values [2.0 (2.0), 1.5 (1.5), and 1.0 (1.1) eV], but the MP2/EC (and MP2/SDB) values [1.5 (1.8), 1.0 (1.2), and 0.6 (0.7) eV] are highly underestimated. Thus, BPW results are much more reliable than MP2 results for the given basis sets.

The experimental bond lengths (r) for Au_2, AuAg, and Ag_2 are 2.47, 2.50, and 2.48−2.53 Å;[12,15,16] the BPW/EC (and BPW/SDB) values are 2.55 (2.54), 2.57 (2.55), and 2.58 (2.57) Å; the MP2/EC (and MP2/SDB) values are 2.53 (2.47), 2.58 (2.49), and 2.62 (2.50) Å. For Au_2^- and Ag_2^-, the experimental r's are 2.58 and 2.60 Å;[12] the BPW/EC (and BPW/SDB) values are 2.67 (2.66) and 2.69 (2.70) eV; the MP2/EC (and MP2/SDB) values are 2.62 (2.56) and 2.75 (2.60) eV. The MP2/SDB bond lengths show good agreements with the experimental values. The BPW bond lengths for the dimer system are slightly longer than the experimental values (by less than 0.1 Å), but the deviation is consistent for both Au, Ag, and alloy systems.

From these results, we note that both BPW/EC and BPW/SDB results are similar and in good agreement with the experimental electronic properties. On the other hand, in the case of MP2/SDB calculations, though the bond distances are in good agreement with the experimental values, the EAs and IPs are too small and the dissociation energies are overestimated. Therefore, it is expected that BPW/SDB would give the most reliable electronic properties and energetics for the alloy clusters among the two BPW methods and two MP2 methods employed, while BPW/EC results are very similar to the BPW/SDB results. Since BPW/SDB calculations require much more computing time than BPW/EC calculations, BPW/SDB calculations are not practical for large cluster systems. Thus, for comparison of diverse clusters of pure Au_k, pure Ag_k, and binary Au_mAg_k systems as well as for thorough search for these lowest energy structures, we used BPW/EC results. Indeed, we note that the BPW/EC results are in good agreement with the results of small gold and silver clusters (for $k \leq 3$) calculated at the high levels of theory (CCSD and CCSD(T)),[18a] which is in excellent agreement with experiment. The BPW/EC VDEs of small binary gold−silver clusters Au_mAg_n ($3 \leq k \leq 4$) are also in good agreement with the experimental values, which will be discussed later. However, the bond lengths predicted by BPW/EC calculations need to be shortened by 0.1 Å so as to be more realistic.

B. Pure Gold/Silver Clusters vs Gold−Silver Binary Clusters: Origin of Alloy Formation. To investigate the gold−silver binary systems, it is important to understand the origin of alloy formation from the comparison of the binary systems with the pure systems. To this end, we investigate the stability of pure and binary clusters using molecular orbital (MO) analysis of the dimer and trimer systems.

Figure 1 shows the schematics of MO energies for neutral dimer clusters. The Au atom has 6s and 5d orbital energies equal to −6.05 and −7.04 eV, respectively, while the Ag atom's 5s and 4d orbital energies are −4.69 and −7.22 eV, respectively. Since the s orbital of Au is much lower in energy than that of Ag atom, the IPs and VDEs of Au_k clusters tend to be larger than those of Ag_k clusters. In contrast to a large energy gap (2.53 eV) between 5s and 4d orbitals in the Ag atom, the Au atom has a small energy gap (0.99 eV) between 6s and 5d orbitals which is known to be due to the relativistic effect in Au.[33]

It is clear that the highest occupied molecular orbital (HOMO) of AuAg is between the HOMOs of Au_2 and Ag_2 but much closer to that of Au_2. The experimental D_0 ($2D_0^*$) of Au_2, AuAg, and Ag_2 are 2.29, 2.08, and 1.65 eV, respectively,[12,13] and the corresponding D_0' ($2D_0^{*\prime}$) of Au_2^-, $AuAg^-$, and Ag_2^- are 1.92, 1.08, and 1.37 eV, respectively.[12,14] Although Au tends to bind Ag with large D_0, the stability of AuAg over Au_2 and Ag_2 is not clear. However, the partial electron transfer from Ag to Au

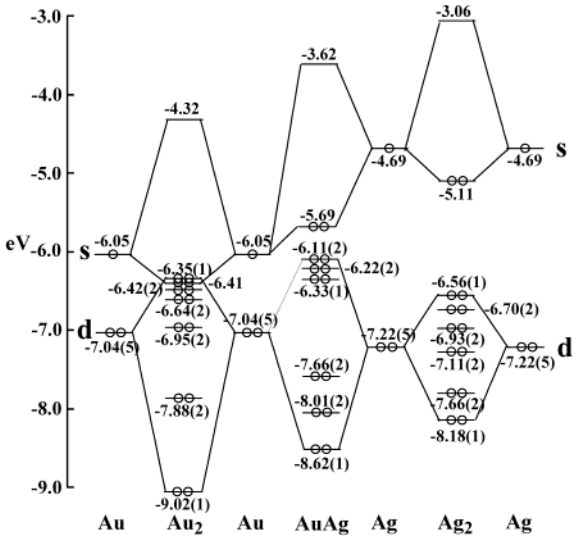

Figure 1. MO energies of Au_2, AuAg, and Ag_2. The occupied electrons are shown as circles. The value in parentheses is the number of degenerate states of the d-orbital type MOs.

(i.e., partial charge transfer from Au to Ag) gives a clear picture of stability of binary neutral clusters, which will be discussed below.

In the case of Au_2, the 6s orbitals (−6.05 eV) of two Au atoms interact with each other to form a bonding MO (−6.35 eV) and an antibonding MO (−4.32 eV). In the case of Ag_2, the two s orbitals (−4.69 eV) form the bonding and antibonding MOs (−5.11 and −3.06 eV), respectively. On the other hand, in the case of AuAg, the large difference in s orbital energy between Au and Ag makes the binary dimer form a charge-complex (but not an ionic system due to the lack of full charge transfer) by partial charge transfer from Au to Ag. Thus, the bonding MO (−5.69 eV) is similar to the s orbital of Au (or bonding orbital of of Au_2), while the antibonding MO (−3.62 eV) is similar to the antibonding MO of Ag_2. This results in stabilization of the AuAg alloy but much less stabilization of the $AuAg^-$ alloy, which can reasonably explain the experimental and calculated dissociation energies of these dimeric systems.

Since the s−d orbital energy separation in Au_2 is small, the d orbitals form five bonding MOs (−9.02, −7.88, −7.88, −6.95, −6.95 eV) and five antibonding MOs (−6.64, −6.64, −6.42, −6.42, −6.35 eV), which can be compared with the s-type bonding MO (−6.41 eV). Thus, significant mixing between s and d orbitals (s−d hybridization) arises in Au_k clusters, which is not possible in Ag_k clusters since the lowest s-type orbital energy (−5.11 eV) is much higher than the highest d-type orbital energy (−6.56 eV). In the case of AuAg, the lowest s-type orbital energy (−5.69 eV) is only slightly higher than the highest d-type orbital energy (−6.11 eV). Therefore, in the Au_mAg_n clusters, the s−d hybridization would be possible depending on the composition ratio of Au to Ag.

The partial charge transfer and s−d hybridization are clear from Figures 2 and 3 which show MOs of the neutral and anionic dimer and trimer systems, respectively. The HOMO of Au_2 is an s−d hybrid antibonding orbital (the 2nd HOMO is an s-type bonding orbital), while the HOMO of Ag_2 is simply an s-type bonding orbital. The partial charge transfer in AuAg is clearly seen in Figure 2. The natural bond orbital (NBO) atomic charges of Au and Ag are −0.27 and 0.27 au, respectively, which results in electrostatic energy gain. This, in turn, results in enhanced binding energy (per atom) [0.99 eV for AuAg, which is larger than the mid value (0.92 eV) between the binding energy of Au_2 (1.03 eV) and that of Ag_2 (0.82 eV)].

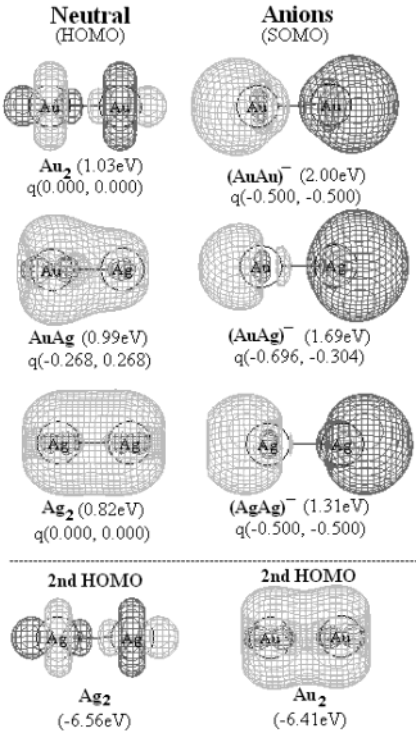

Figure 2. MOs of pure and binary dimer clusters (both neutral and anions). The value in parentheses is the dissociation energy per atom (D_0^*), and q is the NBO charge (in au).

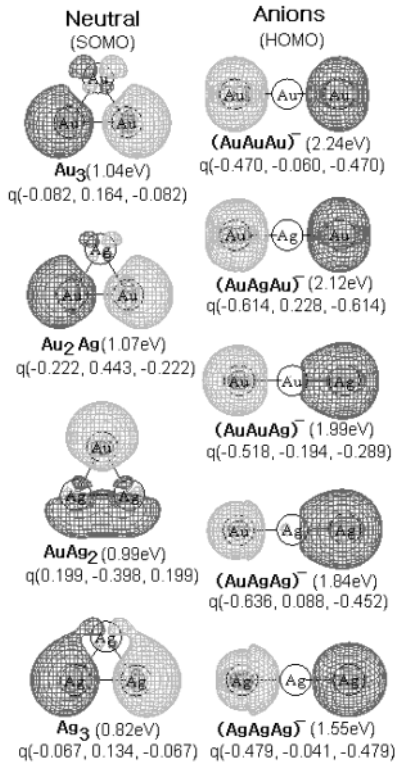

Figure 3. Molecular orbital picture of pure and binary trimer clusters (both neutral and anions). The value in the parentheses is the dissociation energy per atom (D_0^*), and q is the NBO charge (in au).

A similar trend is noted in the cases of Au_2Ag and $AuAg_2$ with large electrostatic energy gain in the alloys in comparison with the cases of Au_3 and Ag_3 (Figure 3). The dissociation energies per atom of Au_3, Au_2Ag, $AuAg_2$, and Ag_3 are predicted to be 1.04, 1.07, 0.99, and 0.82 eV, respectively. It is interesting to note that the binding energy of Au_2Ag is larger than that of Au_3. In consideration of the percentage of Au and Ag atoms, the interpolated binding energies of Au_2Ag and $AuAg_2$, in the absence of extra electrostatic energy gain due to the partial charge transfer, are expected to be 0.97 and 0.89 eV, respectively. Therefore, the relative energy gains for the formation of both Au_2Ag and $AuAg_2$ are considered to be 0.10 eV. The energy gain for Au_2Ag should arise from the large electrostatic interactions between two Au−Ag pairs and the small electrostatic repulsion for the Au−Au pair (the charges of Au and Ag are −0.22 and 0.44 au, respectively). Similarly, the energy gain for Au_2Ag_2 should arise from the large electrostatic interactions between two Au−Ag pairs and the small electrostatic repulsion for the Ag−Ag pair (the charges of Au and Ag are −0.40 and 0.20 au, respectively).

The s−d hybridization should play an important role in determining the structure of clusters. Owing to this s−d hybridization, Au_k clusters can easily form linear and planar structures. On the other hand, the s orbitals of Ag_k clusters tend to form spherical structures toward the 3-D structures. This trend is indeed found in the pure gold and silver clusters. Thus, the ratio of Au to Ag atoms governs the structure of the binary clusters. In the case of neutral Au_mAg_n clusters, the partial charge transfer from Au to Ag (Au tends to be negatively charged, while Ag is positively charged) is clearly noted. This results in electrostatic energy gain for binary Au_mAg_n clusters over pure Ag_k and Au_k clusters.

In the case of anionic dimer clusters (both pure and binary), the charges on Au and Ag are all negative which makes the electrostatic energy gain less favorable for these systems. The partial charge transfer is also noted in these anionic systems to reduce the electrostatic repulsions between two charges with the same signs as well as to gain the electrostatic energy between two charges with opposite signs. However, the charges of Au and Ag in $AuAg^-$ are −0.70 and −0.30 au, respectively, which results in only slightly reduced electrostatic repulsion over Au_2 and Ag_2 in which both charges are −0.5 au. In the anionic trimer clusters Au_3^-, Ag_3^-, $AuAuAg^-$, and $AgAuAg^-$, all atomic charges are negative (Figure 3). On the other hand, in the cases of $AuAgAu^-$ and $AuAgAg^-$, the central atom has opposite charge to the terminal atoms. Thus, these species which are stabilized by strong electrostatic energy gain are more stable than $AuAuAg^-$ and $AgAuAg^-$, respectively. Such electrostatic energy gain should be responsible for alloy formation, which is corroborated by comparing the dissociation energies of binary clusters with respect to the interpolated dissociation energies between pure Au_m and pure Ag_n clusters. (This will be discussed later.)

When the cluster size increases, the orbital mixing is much more complicated, and so the analysis is less clear. Nevertheless, in the neutral systems, the bonding character tends to be enhanced with increasing cluster size, and the large dissociation energy for the alloy formation can be easily understood. In the case of large anion systems, the HOMO−LUMO energy gaps become smaller, and so the destabilization effect by an extra electron is lessened. Thus, the dissociation energy gain by alloy formation tends to increase as the extra electron occupies the second lowest energy state among a number of bonding-type orbitals. Eventually, as the cluster size becomes large, the distinction in alloy formation between the neutral and anionic systems becomes insignificant.

Since the s−d hybridization plays an important role in governing the structure of clusters, the accurate evaluation of the s−d energy gaps is important. However, it is well-known that in DFT calculations, HOMO−LUMO energy gaps tend to

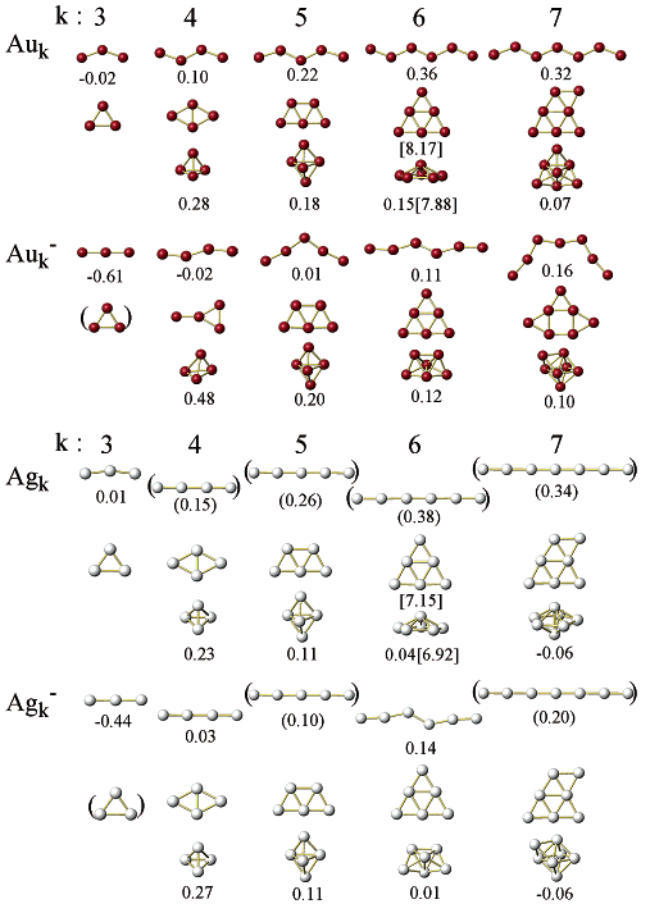

Figure 4. Structures and relative energies (in eV/atom with respect to the 2-D lowest energy structure) of neutral and anionic gold and silver clusters ($k = 3-7$). The values in parentheses indicate the relative energies for the symmetry constraint structures in parentheses. The bracketed values are IP_v.

be underestimated (e.g., s−d orbital energy gap obtained from $d^{10}s^1$ and d^9s^2 electron configurations of Au^-/Ag^-: 1.34/3.94 eV in experiment,[34] 0.46/1.68 eV at DFT, 4.22/7.27 eV at MP2), and thus the s−d hybridization in Au_k clusters can be exaggerated. Therefore, we do not exclude the possibility that the present calculations could be biased in favor of the 1-D and 2-D structures over 3-D structures. Such cases were indeed noted in the water hexamer involving s−p hybridization for which DFT calculations favor 2-D structures, in contrast to the experimental 3-D structure.[35] However, these cases have been limited to the nearly isoenergetic conformers. Indeed, we find that coupled cluster theory with single and double excitations (CCSD) confirms that the DFT calculations are reliable except for the nearly isoenergetic trimer, while the CCSD stability of the 2-D structure over the 3-D structure is somewhat less than the DFT stability.

C. Pure Neutral and Anionic Gold and Silver Clusters ($k \leq 13$). To investigate the Au_mAg_n ($m.n$) binary systems, it is essential to know the structures of pure gold and silver clusters. The lowest energy structures and their relative energies (eV per atom) of the 1-, 2-, and 3-D pure Au_k ($k.0$) and Ag_k ($0.k$) clusters are shown in Figure 4 for $3 \leq k \leq 7$. Table 2 lists the vertical ionization potential (IP_v), VDE, and D_0^* of the pure Au_k and Ag_k clusters, and it can be noted that the calculated and experimental IP_v and VDE are in good agreement except that the IP_v of Au are consistently ∼0.5 eV smaller than the corresponding experimental values possibly due to the lack of explicit relativistic effect (though the relativistic effect was implicitly taken into account using basis sets).

TABLE 2: Comparison of Calculated (BPW/EC) and Experimental Vertical Ionization Potentials (IP_v in eV), Dissociation Energies per Atom (D_0^*) in eV, and Vertical Detachment Energies (VDE, in eV) of Neutral and Anionic Pure Gold (Au_k) and Silver (Ag_k) Clusters[a]

clusters	IP_v		D_0^*	clusters	VDE		D_0^*
($m.n$)	calcd	expt	calcd	($m.n$)	calcd	expt	calcd
Au_3 (3.0)	7.21	7.5	1.04	Au_3^- (3.0)	3.60	3.85	2.24
Au_4 (4.0)	7.9	8.6	1.37	Au_4^- (4.0)	2.75 (2-D)	2.77	2.04
					3.33 (1-D)		2.05
Au_5 (5.0)	7.5	8.0	1.50	Au_5^- (5.0)	3.06	3.12	2.12
Au_6 (6.0)	8.17 (2-D)	8.8	1.73	Au_6^- (6.0)	2.24	2.0	2.09
	7.88 (3-D)						
Au_7 (7.0)	7.18	7.8	1.68	Au_7^- (7.0)	3.43	3.35	2.15
Ag_3 (0.3)	6.00	6.20	0.82	Ag_3^- (0.3)	2.24[a]	2.43	1.55
Ag_4 (0.4)	6.60	6.65	1.08	Ag_4^- (0.4)	1.70	1.65	1.50
Ag_5 (0.5)	6.28	6.35	1.19	Ag_5^- (0.5)	2.07	2.11	1.60
Ag_6 (0.6)	7.15 (2-D)	7.15	1.36	Ag_6^- (0.6)	2.12 (3-D)	2.06	1.58
	6.92 (3-D)				1.40 (2-D)		1.58
Ag_7 (0.7)	6.03	6.40	1.38	Ag_7^- (0.7)	2.60	2.55	1.68

[a] In our previous CCSD and CCSD(T) calculations (ref 18a) using large basis sets including f functions, the VDE as 2.19 and 2.33 eV, respectively. The IP_v's of Au should have a large relativistic effect which we have taken into account in terms of the basis set. Since the effect was not explicitly taken into account, the predicted values for IP_v of Au_k seem to be underestimated (∼0.5 eV smaller than the experimental values), while those of Ag_k are in good agreement with the experimental values. Experimental values are from refs 11 and 12. IP_v of Ag_7 by one-photon ionization experiment was reported as 5.69 eV (ref 11b).

In the case of neutral Au_3 and Ag_3, we find that the energy difference between the triangle and linear structures is very small, because the potential energy is almost constant for the variation of bond angles from 50° to 180°. For Ag_3, the triangular structure is the lowest energy conformer, which is 0.03 eV lower than the linear structure. In the case of Au_3, the linear-like structure with the bond angle of ∼120° is nearly isoenergetic to the triangular structure. The DFT results slightly favor the linear structures, while the MP2 and CCSD results slightly favor the triangular structure. Since the s−d orbital energy separation tends to be underestimated in DFT calculations, the stability of the linear structure for Au_3 seems to be slightly exaggerated. On the other hand, in the anionic Au_3^- and Ag_3^-, the linear structure is much more stable (by 1.8 eV for Au_3^- and by 1.3 eV for Ag_3^-) than the triangular structure in which the extra electron occupies the antibonding orbital according to the Hückel MO theory.

In the neutral systems, both gold and silver clusters up to the hexamer have the same conformational structures, as shown in Figure 4: D_{2h} rhombus for the tetramer, C_{2v} planar trapezoid for the pentamer, and planar D_{3h} triangular structure for the hexamer. However, in the case of heptamer, the silver cluster has a pentagonal bipyramid (PBP) nonplanar structure, while the gold cluster still favors a planar structure. In the anionic systems, gold and silver clusters have different conformational structures except for the trimer (linear structure; $D_{\infty h}$), the pentamer (planar trapezoid), and the hexamer (planar triangular structure). The anionic silver tetramer has the planar rhombus structure, while the anionic gold tetramer has two almost isoenergetic structures viz. zigzag shape (C_{2h}) and T-shape (C_{2v}). This zigzag structure is interesting, because a similar size of gold wire has been studied in experiments.[36] The silver hexamer has two almost isoenergetic isomers, a planar D_{3h} structure and a 3-D C_{2v} structure with a deformed tetrahedral subunit capped by two atoms, while in the gold hexamer, the planar triangular structure is more stable than the 3-D structure. The silver heptamer has the 3-D structure [capped trigonal antiprism (CTA;

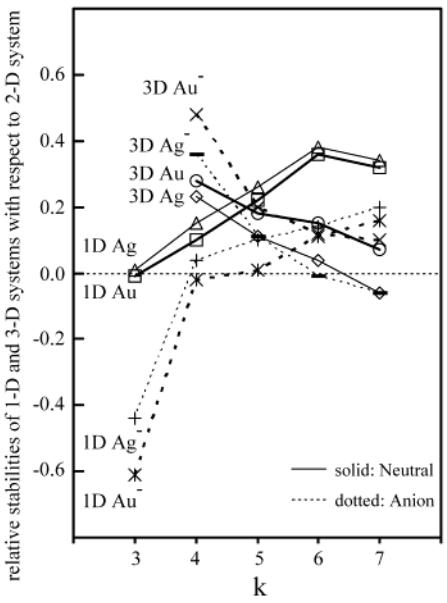

Figure 5. Stability (in eV/atom) of 1-D and 3-D structures relative to the 2-D structure (with respect to the cluster size k) for the neutral and anionic Au_k and Ag_k clusters.

C_{3v})], while the gold heptamer has still the 2-D structure. Our results for silver clusters are in good agreement with that of Fournier and co-workers[21] and also in reasonable agreement with the work of Koutecky and co-workers.[20] Our calculated results for gold clusters are in good agreement with the BO-LSD-MD results of Landman and co-workers.[23]

In our calculations, small-size pure neutral Au_k and Ag_k clusters (for $k \leq 6$) have 2-D structures, and the 2-D structure continues to be favored in the Au_k clusters (at least up to $k = 13$), whereas in the Ag_k clusters, the 3-D structure becomes more stable from the heptamer ($k = 7$). Thus, it is interesting to compare the stabilities of 1-D, 2-D, and 3-D structures of neutral and anionic gold and silver clusters, which we show in Figures 4 and 5 (for $3 \leq k \leq 7$). As the cluster size increases, 3-D structures get stabilized for both gold and silver. Nevertheless, the gold clusters tend to keep 2-D structures even for $k = 7$, while the silver clusters have already 3-D structures for $k = 7$. The anionic systems tend to stabilize 1-D structures much more than the neutral systems do, which is much more pronounced in the case of gold clusters. The linear chain structure of Au_4^- is lower in energy by 0.05 eV than the 2-D T-shape structure, whereas the linear structure of Au_4 is higher in energy by 0.39 eV than the 2-D rhombus structure. The linear chain structure of Ag_4^- is higher in energy by 0.12 eV than the 2-D rhombus structure, while the linear structure of Ag_4 is higher in energy by 0.62 eV than the 2-D structure. The linear chain structures of neutral Au_k are found to be at the local minima on the energy potential surface. These anionic states are much better stabilized by the extra electron. In this case, the terminal atoms are negatively charged, with the alternations of positive and negative charges between neighboring Au atoms (e.g., atomic charges of a linear Au_7: −0.036, 0.032, −0.006, 0.019, −0.006, 0.032, −0.036 au in the order). This results in electrostatic interaction energy gain in the linear chain structure. The linear structure was stabilized due to the s−d hybridization in Au_k clusters. On the other hand, in the case of linear Ag_k, the terminal atoms are positively charged, while the negative charges are distributed over central atoms (e.g., atomic charges of the linearly constrained structure of Ag_7: 0.119, −0.031, −0.046, −0.083, −0.046, −0.031, 0.119 au in the order). In this case, the overall electrostatic energy gain is small.

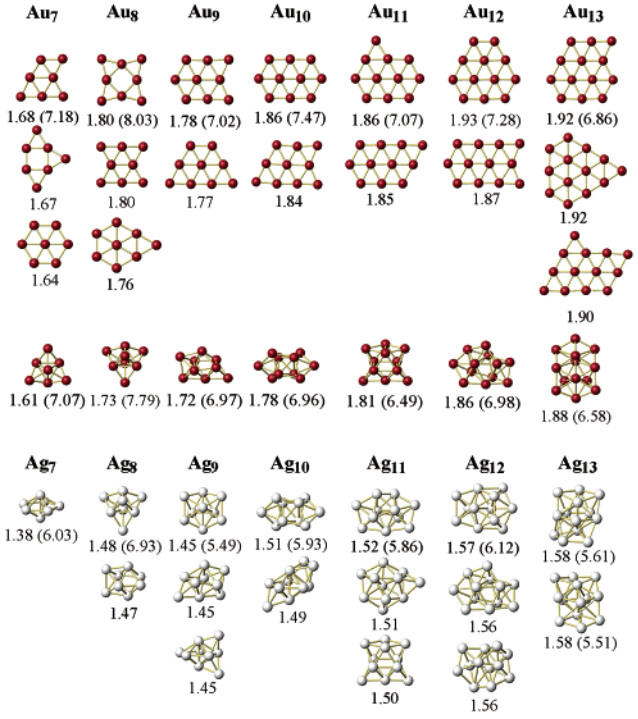

Figure 6. Structures of neutral gold and silver clusters ($k = 7-13$). The ZPE-corrected dissociation energy (eV/atom) is given below each cluster, and the IP_v value (eV) is in parentheses. Nearly isoenergetic lowest energy structures are given: In the gold clusters, the 3-D structures are additionally given for comparison.

Au_k clusters tend to have 2-D structures (and even 1-D structures are reasonably stable), while Ag_k clusters favor the 3-D structures. Thus, the coordination number (Nc) of each Au atom is rather small compared with that of Ag atom. As the anionic systems tend to stabilize the 1-D structures as well as 2-D structures much more than the neutral systems, the Nc tends to be smaller than in the neutrals. This trend provides useful information of the structure for large size gold−silver alloy clusters. For example, the largest Nc of Ag_7 is 6, while that of Ag_7^- is 5; the largest Nc of Au_7 is 5, while that of Au_7^- is 4 (Figure 4).

It is well-known that the observed VDE (as well as IP) of the small metal and nonmetal clusters is very sensitive to their structures.[20−23,37] Such sensitive change in VDE of the isomeric structures of both gold and silver anionic clusters is also noted in the present system. For Au_4^-, our calculated VDEs of T-shaped (C_{2v}) and zigzag (C_{2h}) structures are 2.75 and 3.33 eV, respectively. With BO-LSD-MD calculation, Landman[23] reported these values as 2.78 and 3.30 eV, respectively, while Andreoni,[22] using BLYP with plane waves, reported these values as 2.78 and 3.39 eV, respectively. All the calculated results imply that only a T-shaped (C_{2v}) isomer can contribute to the detachment threshold (2.77 eV) in the PES spectrum of Au_4^-.[12] The same situation appears in Ag_6^-; the calculated VDEs of the 2-D D_{3h} and 3-D C_{2v} structures are 1.40 and 2.12 eV, respectively. The experimental VDE value is 2.06 eV.[12] Thus, it is likely that the 3-D C_{2v} structure was observed in the experiment.

As 2-D structures are more stable than 3-D in Au_k clusters for up to $k = 7$, we have further investigated the lowest-energy structures of neutral pure gold and silver clusters ($k = 7-13$), which are shown in Figure 6. The lowest neutral gold clusters have 2-D planar structures, in contrast to the recently predicted 3-D structures.[39d] The lowest-energy silver heptamer is pen-

TABLE 3: 2-D and 3-D Relative Stabilities (eV) of Neutral Silver and Gold Clusters[a]

cluster		BPW/EC	MP2/SDB	CCSD/SDB
Au_3	1-D	−0.10	0.18	0.06
	2-D	0.00	0.00	0.00
Au_4	1-D	0.39	0.98	0.63
	2-D	0.00	0.00	0.00
Au_6	2-D	0.00	0.00	
	3-D	0.89	0.65	
Au_8	2-D	0.00	0.00	0.00
	3-D	0.51	−1.15	0.18
Ag_3	1-D	0.03	0.20	0.12
	2-D	0.00	0.00	0.00
Ag_4	1-D	0.62	1.20	0.84
	2-D	0.00	0.00	0.00
Ag_6	2-D	0.00	0.00	0.00
	3-D	0.25	−0.04	0.21

[a] CCSD energies were calculated at the MP2/SDB geometries.

tagonal bipyramidal (PBP) structure. The octamer is an extended tetrahedral (T_d) structure, which does not have the PBP moiety. However, the structures of silver nonamer ($k = 9$) to tridecamer ($k = 13$) have the PBP moiety. The present results (Figures 4 and 6) can be compared with the previously reported structures for $k = 3-12$.[21] The relative stabilities of the pure neutral gold and silver clusters were recompared at the MP2 and CCSD levels of theory using the SDB pseudopotentials and (8s7p6d2f)/[6s5p3d2f] basis set at the MP2-optimized geometries (Table 3). Between BPW and MP2 calculations, the BPW calculations show more reliable electronic properties of gold and silver clusters, whereas the MP2 calculations give more reliable optimized geometries (at least for the dimeric systems). The Au_3 and Ag_3 cyclic ring conformers of 2-D structure are more stable by 0.18 and 0.20 eV than the linear 1-D structures at the MP2 level, and by 0.06 and 0.12 eV at the CCSD level. At the BPW/MP2/CCSD levels, 2-D structures of Au_4 and Ag_4 are 0.39/0.98/0.63 and 0.62/1.20/0.84 eV more stable than the corresponding 1-D structures, respectively, and 2-D structures of Au_6, Au_8, and Ag_6 are 0.89/0.65/−, 0.51/−1.15/0.18, and 0.25/−0.04/0.21 eV more stable than the corresponding 3-D structures, respectively. In comparison with the CCSD calculations, the MP2 calculations tend to slightly more stabilize higher dimensional structures, whereas the BPW calculations tend to slightly more stabilize lower dimensional structures. Nevertheless, the overall trend of the BPW results is consistent with that of the CCSD results for these small metal clusters. For small neutral gold ($k \leq 13$) and silver ($k \leq 6$) clusters, 2-D structures are slightly more stable than 3-D structures for both BPW and CCSD calculations. However, in the MP2 calculations, 3-D structures of Au_8 and Ag_6 are 1.15 and 0.04 eV more stabilized than the corresponding 2-D structures, respectively, possibly due to the exaggerated HOMO−LUMO energy gap (whereas at the BPW/CCSD level, the two 2-D structures are more stabilized than the corresponding 3-D structures by 0.51/0.18 and 0.25/0.21 eV, respectively). Since the CCSD results are known to be very reliable, we thus believe that the energetics and electronic properties of gold and silver clusters were somewhat reliably produced at the BPW calculation level (much better than the MP2 level). We also note that the IP_vs of 2-D gold clusters are closer to the experimental values than those of 3-D structures, as shown in Figure 6. It was reported that the 2-D anionic gold clusters are more stable than the 3-D ones up to $k = 13$ at the DFT level.[39b] This is evident from our results of the neural species because the anionic systems tend to stabilize lower dimensional structures more than the neutral systems. As the number of atoms increases, the difference between the neutral and anionic species decreases, because the effect of the excess electron decreases as the charge density per atom decreases.

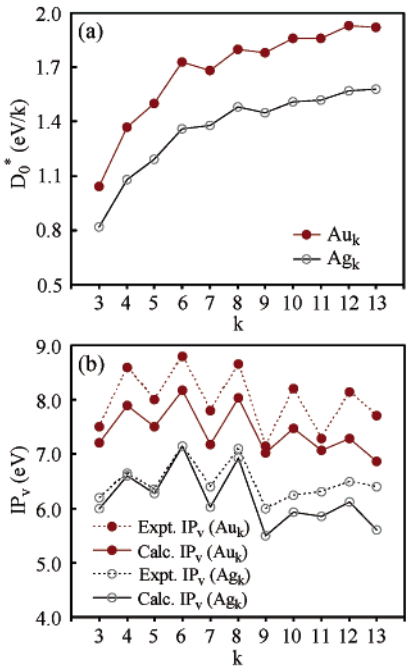

Figure 7. (a) The ZPE-corrected dissociation energy per atom (D_0^*) of neutral gold and silver clusters ($k = 3-13$) and (b) their IP_vs.

Figure 7 shows the good agreement between experimental and calculated results of D_0^*s and IP_vs of the pure gold and silver trimer to tridecamer ($k = 3-13$). The IPs are slightly underestimated in comparison with the experimental values possibly due to the underestimated HOMO−LUMO energy gap in the DFT calculations. The odd−even oscillation behavior appears for IP_vs and EA_vs, and the successive binding energies are large for the changes from the odd to even k.

D. Gold−Silver Binary Clusters ($3 \leq k \leq 7$). To search for the lowest energy structures of gold−silver alloy clusters for $k \leq 3$, we considered various topologically different conformers, as in our previous search approach used in finding the water clusters wherein we considered nearly 1000 conformers for 41 topologically different types.[38] A thorough search for the lowest energy structures of the Au_mAg_n binary clusters was done, and these structures were fully optimized. Starting from more than 2000 different initial conformations based on different topological structures for each k-membered clusters, we found more than 270 local minima for neutral and anionic gold−silver binary clusters ($3 \leq k \leq 7$). The most stable structures of neutral and anionic binary clusters along with their IP_v or VDE and D_0^* are in Figures 8 and 9. The calculated VDEs for $3 \leq k \leq 4$ (including the BPW/SDB calculations) are compared with the experimental values in Table 4. We adopt a label "*m.n.x*", where m and n denote the numbers of gold and silver atoms in the cluster, respectively, while x (= *a*, *b*, *c*, ...) denotes the rank in the increasing energy order (e.g., $x = a$ and *b* indicate the lowest and the second lowest structure, respectively). In the case of lowest energy structures, the notation "*a*" is omitted for clarity. Note that some clusters such as $Au_2Ag_2^-$, $AuAg_3^-$, and $AuAg_6^-$ have two isoenergetic structures.

Since the IP_v of Au is larger than that of Ag, the IP_v in the binary clusters tends to increase with an increasing number of Au atoms.[17] Exceptionally, the triangular Au_3Ag_3 (3.3) binary system has the largest IP_v (8.97 eV) among the considered small clusters possibly due to the high stabilization (with negatively charged Au atoms outside and positively charged Ag atoms

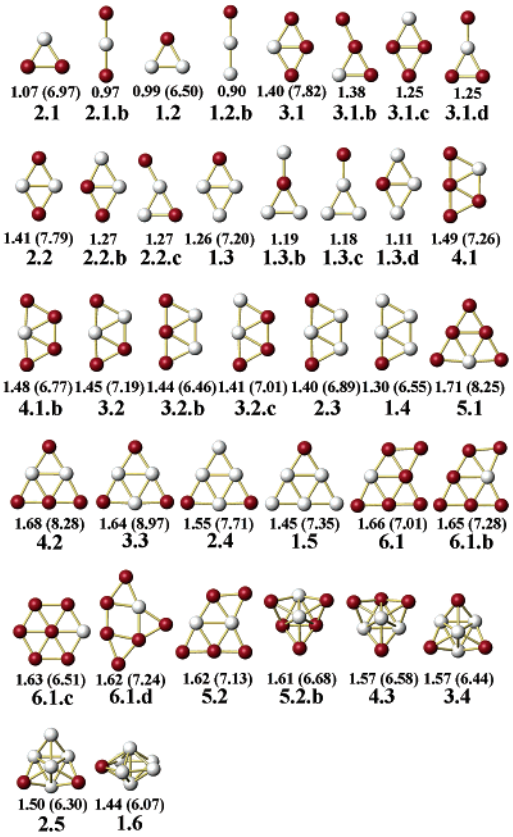

Figure 8. Optimized structures of neutral binary Au_mAg_n clusters (*m*.*n*). The black and white spheres represent gold and silver atoms, respectively. The dissociation energy (D_0^*; eV/atom) is given below each figure, and the vertical IP (IP_v; eV) is given in parentheses.

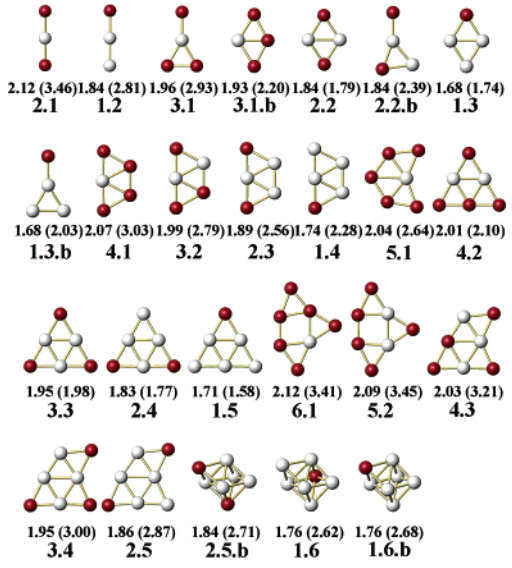

Figure 9. Optimized structures of anionic binary $Au_mAg_n^-$ clusters (*m*.*n*). The black and white spheres represent gold and silver atoms, respectively. The dissociation energy (D_0^*; eV/atom) is given below each figure, and the VDE (VDE; eV) is given in parentheses.

inside) by effective partial charge transfer from Au atoms to Ag atoms. In addition, these triangular hexamer clusters also give the largest IP_v in the considered small pure gold and silver clusters. The VDE tends to increase with the cluster size. In the binary systems, the VDE tends to increase with the number of Au atoms for the given size. However, the VDE strongly depends on the structure, in particular, in small clusters.

TABLE 4: Comparison of Calculated and Experimental Vertical Detachment Energies (VDE in eV) and Calculated Dissociation Energy per Atom (D_0^*) in eV) of Anionic $Au_mAg_n^-$ ($3 \le m + n \le 4$) Clusters

clusters	calcd VDE	expt VDE[a]	D_0^*
3.0	3.60	3.85	2.24
2.1	3.46(3.50)	3.86 ± 0.01	2.12
2.1.b	2.93		1.99
1.2	2.81(2.90)	2.97 ± 0.02	1.84
1.2.b	2.31		1.74
0.3	2.24	2.43	1.55
4.0	2.75	2.77	2.04
3.1	2.93(2.93)	3.00 ± 0.06	1.96
2.2	1.79(1.82)	1.62 ± 0.03	1.84
2.2.b	2.39(2.41)	2.36 ± 0.06	1.84
1.3	1.74(1.78)	1.66 ± 0.02	1.68
1.3.b	2.03(2.06)	2.03 ± 0.03	1.68
0.4	1.70	1.65	1.50

[a] The calculated values were obtained using BPW/EC pseudopotentials (and BPW/SDB pseudopotentials in parentheses). Experimental values are from ref 14.

Tables 1−3 list the calculated and experimental data (IP_v and VDE) for low-energy conformers. In Figures 4, 6, 8, and 9, the calculated IP_vs and VDEs are listed in parentheses including dissociation energies D_0^*. The experimental values (IP_v for neutral state and VDE for anionic state) are available for the pure systems ($k \le 7$). However, the experimental values of the binary systems are available up to $k = 4$. Our results are in good agreement with the available experimental data.

We note that the cluster stability is governed mostly by the following trends: (i) higher Nc in spherical coordination for Ag atoms and smaller Nc in 1-D or 2-D coordination for Au atoms, (ii) larger electrostatic interaction energy gain by partial charge transfer (from Au to Ag), and (iii) the tendency that Au atoms tend to be on the surface/edges/vertices with negative charges, while the Ag atoms tend to be inside with positive charges. These trends are more notable in the anionic systems. We note that, for example, in both neutral and anionic Au_3Ag_3, Au atoms are located on the outside (i.e., vertices) of the triangle with smaller Nc and negative charges, while Ag atoms are inside the triangle with larger Nc and positive charges. It is also interesting to note that for $k = 7$, the structures of binary clusters 6.1, 5.2, 4.3, and 2.5, are planar (like pure gold clusters), while 1.6 which requires high Nc shows 3-D structure (like pure silver clusters), as shown in Figures 8 and 9. It is noted that 6.1b with Nc(Ag) = 5 is nearly isoenergetic to 6.1 with Nc(Ag) = 4 from Figure 8. The Nc = 5 for Ag would not be so favorable because this coordination is restricted to the plane, while Ag tends to have large Nc by spherical coordination. A similar case is also found for the another nearly isoenergetic conformer 6.1c in which one Ag atom is not inside but outside because the coordination number 6 for the Ag atom should not be restricted to the plane.

In the case of anion, Au−Ag−Au^- (2.1) and Au−Ag−Ag^- (1.2) are lower in energy than Au−Au−Ag^- and Ag−Au−Ag^-, respectively. It is easy to find that the structures with Au atoms separated by Ag atoms are effectively stabilized with enhanced binding energies (cohesive energies) by the electrostatic interactions between neighboring atoms.

The predicted vertical ionization potential (IP_v) energies of various isomers of neutral Au_mAg_n clusters ($3 \le k = m + n \le 7$) are given in Figure 8, and the predicted VDEs of the anionic $Au_mAg_n^-$ clusters are given in Figure 9. Our calculated VDEs for small binary anionic gold−silver clusters $Au_mAg_n^-$ ($2 \le k = m + n \le 4$) as well as for pure gold and silver clusters are in good agreement with available experimental results[14] (see

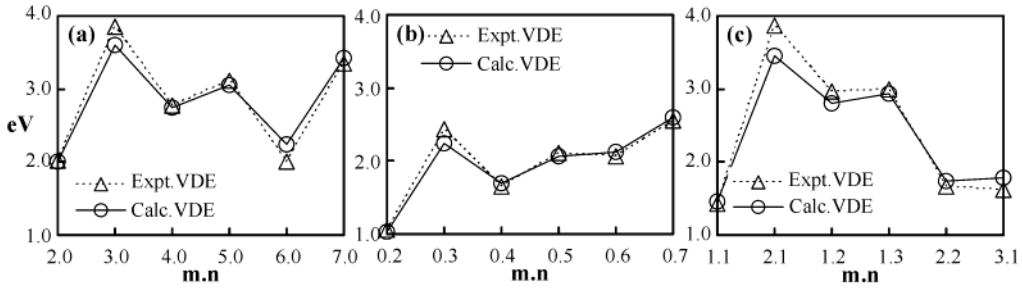

Figure 10. Calculated (open circles) and experimentally measured (open triangles) VDE for (a) gold, (b) silver, and (c) gold−silver binary anion clusters. (1.1, 2.1, ... denote the lowest energy structures.)

Figure 10). For some larger clusters, there are several low-lying energy isomers such as $AuAg_6^-$; the energy difference of the lowest and the sixth lowest isomers is only 0.07 eV. It is very interesting that, for anionic $Au_2Ag_2^-$ and $AuAg_3^-$ clusters, Nakajima and co-workers[14] observed that the intensity ratio of the PES peaks depends on the ion source conditions, and they suggested that it arises from the coexistence of two isomers. Our results support their prediction, since both anionic $Au_2Ag_2^-$ and $AuAg_3^-$ clusters have two isoenergetic structures (see Figure 9), respectively. The calculated VDEs of the two most stable isomers for $Au_2Ag_2^-$ and $AuAg_3^-$ are also in good agreement with the experimental results (Table 4).

In our calculated results for these binary clusters (Au_mAg_n), the most stable structures of the binary clusters are related to the important low-lying energy structures of pure gold and silver clusters. Metal atoms in anionic clusters have lower coordination numbers than in the neutrals. As the number of Ag atoms increases in the binary systems, the 3-D structures are favored, as in silver clusters. In the most stable structures of these binary clusters, the silver atoms prefer to occupy the sites with more nearest neighbors than gold atoms. The average Nc's of gold and silver atoms in binary Au_mAg_n clusters are defined as the following: average Nc(Au) = $(2 \times N_{Au-Au} + N_{Au-Ag})/m$; average Nc(Ag) = $(2 \times N_{Ag-Ag} + N_{Au-Ag})/n$, where N_{Ag-Ag}, N_{Au-Au}, and N_{Au-Ag} are the number of Ag−Ag, Au−Au, and Au−Ag bonds in the binary Au_mAg_n clusters, respectively. From Figure 11, one can easily note that Nc(Au) is smaller than Nc(Ag) for both neutral and anionic binary clusters, and Nc(Au) in the anionic cluster is in most cases smaller than that in the corresponding neutral cluster. In addition, we note that in almost all cases, the sum of coordination numbers of all Ag and Au atoms in the anionic clusters is smaller or equal to that in the neutral clusters. Indeed, 2-D structures (with small Nc) are more favored in the anionic system than in the neutral system. Neutral 4.3, 3.4, 2.5, and 1.6 conformers favor 3-D structures due to the trend toward the higher Nc for Ag atoms, while their anionic conformers have 2-D structures. These trends are useful for finding the most stable structures of the larger binary gold−silver clusters.

Figure 12(a),(b) shows the stabilities of these binary clusters using the cohesive or dissociation energy per atom (D_0^*) for neutral and anionic Au_mAg_n clusters where $D_0^* = -[E_0(Au_mAg_n) - mE_0(Au) - nE_0(Ag)]/(m+n)$. Since Au_k have stronger binding energies than Ag_k, the stability of the Au_mAg_n cluster [$\Delta D_0^*(Au_mAg_n)$] can be investigated from the deviation from the linear line of $D_0^L(m.n)$ starting from $D_0^*(Au_k)$ to $D_0^*(Ag_k)$, i.e., $D_0^L(m.n) = D_0^*(Au_k) - n\{D_0^*(Au_k) - D_0^*(Ag_k)\}/k$ and $\Delta D_0^*(Au_mAg_n) = D_0^*(Au_mAg_n) - D_0^L(m.n)$. From Figure 12(a), we find that ΔD_0^* is maximized around $k/2$ for the neutral species, while this trend is much less clear in the anionic species possibly due to the presence of the extra electron. The maximized stability for neutral species (Figure 12(a)) is $m = 1$ for $k = 2$, $m = 1$, (2) for $k = 3$, $m = 2$ for $k = 4$, $m = (2)$, 3 for $k = 5$, $m = 3$ for $k = 6$, and $m = 4$ for $k = 7$. This indicates that the Au−Ag alloy is the most stabilized when the compositions of Au and Ag are equal. We will show that the stabilization for alloy formation emerges from electrostatic interactions as a result of significant partial charge transfer from Au to Ag atom. In particular, it is interesting to note that even without considering the interpolated energy, D_0^* of 2.1 (1.07 eV) is larger than those of clusters 3.0 (1.04 eV), 1.2 (0.99 eV), and 0.3 (0.82 eV), and D_0^* of 3.1 (1.40 eV) and 2.2 (1.41 eV) are larger than those of 4.0 (1.37 eV), 1.3 (1.26 eV), and 0.4 (1.08 eV). Alloy 2.1 has some enhanced electrostatic interaction energy gain due to the transferred charge from Au to Ag atom, while alloy 3.0 has a small electrostatic energy gain due to a small partial charge transfer. Similarly, 3.1 and 2.2 have a large electrostatic interaction energy gain in comparison with 4.0. Especially in 2.2, two Ag atoms separating two Au atoms induce the large electrostatic interaction energy gain. Exceptionally, the dissociation energies per atom of 2.1 and 2.2 conformers appear higher than those of pure Au clusters in Figure 12(a).

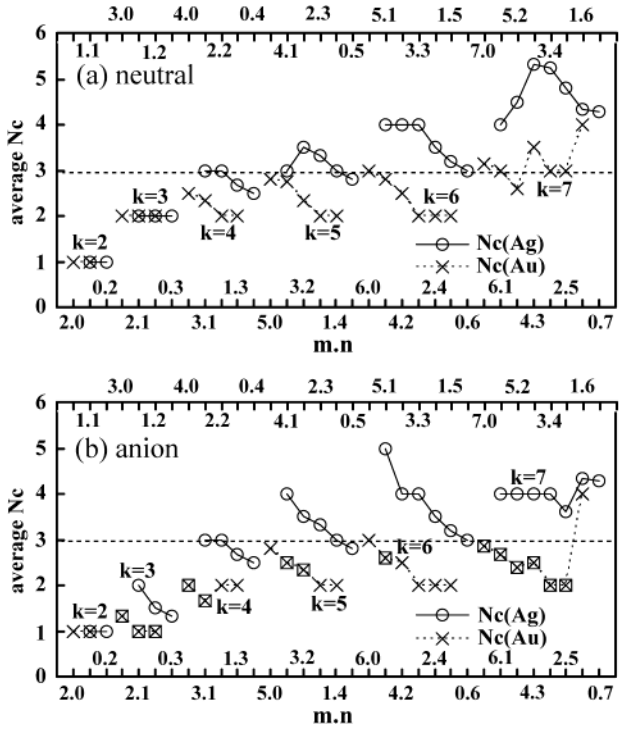

Figure 11. Average coordination numbers (Nc) in the most stable structures of neutral and anionic binary clusters, Au_mAg_n (*m.n*). The scale (*m.n*) is given in the increasing order of $k = m + n$ and the increasing order of n for the given k [(2.0), (1.1), (0.2); (3.0), (2.1), (1.2), (0.3); ...(0.7)]. It can be seen that Nc(Au) tends to be smaller than Nc(Ag). The boxed cross indicates that the Nc(Au) of the anionic state (b) is smaller than that of the corresponding neutral state (a).

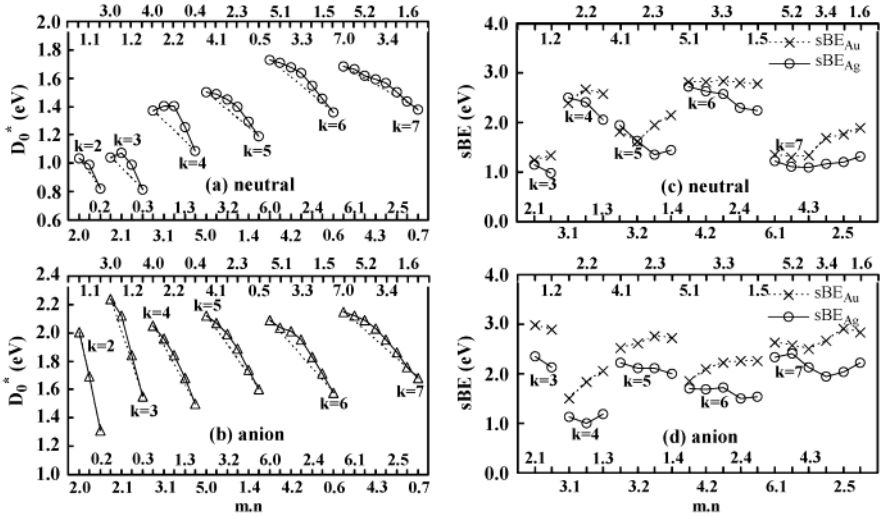

Figure 12. Dissociation energies per atom (D_0^*) (a; neutral and b; anion) and successive binding energies (sBE) (c; neutral and d; anion) of the most stable structures of binary Au_mAg_n ($m.n$) clusters.

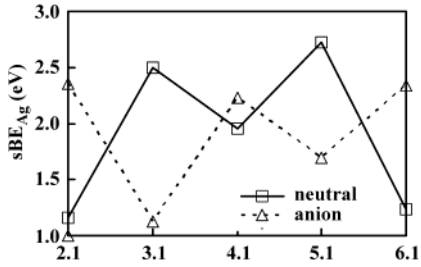

Figure 13. Successive binding energies (sBE_{Ag} and sBE_{Au}) for the binary Au_mAg clusters ($m = 2-6$).

Figure 12(c),(d) shows the successive binding energy (sBE) of these binary clusters. We present two ways of defining sBE: For neutral Au_mAg_n clusters, it is defined as $Au_mAg_n = Au_mAg_{n-1} + Ag - (sBE_{Ag})$ or $Au_mAg_n = Au_{m-1}Ag_n + Au - (sBE_{Au})$, and for anionic Au_mAg_n clusters, the definitions are $Au_mAg_n^- = Au_mAg_{n-1}^- + Ag - (sBE_{Ag})$ or $Au_mAg_n^- = Au_{m-1}Ag_n^- + Au - (sBE_{Au})$. These binary clusters exhibit odd−even oscillation in sBE, as seen in pure gold and silver clusters.[12,23] This is demonstrated for the series of Au_mAg ($m = 2-6$) clusters in Figure 13 (only sBE_{Ag} is displayed for clarity.) Note that the odd−even oscillation features between neutral and anionic binary clusters are opposite, because the closed shell structure is obtained with an even number of electrons with which the electronic repulsions are minimized according to the Pauli exclusion principle.

4. Conclusion

In summary, we have extensively investigated neutral and anionic gold−silver binary clusters as well as pure gold and silver clusters. DFT calculations have been mostly employed, while MP2 and CCSD ab initio calculations were also carried out to test the validity of the DFT results. The calculated IPs, EAs, and VDEs of these clusters are in good agreement with the experimental data. We find several interesting features for the gold and silver nanoparticles, which may serve as a guideline for determining the structures of large binary clusters.

(1) Gold (Au_k) and silver (Ag_k) clusters show the odd−even oscillation for their stability and electronic properties as a function of the number of atoms. In the neutral state, even numbered k tends to be more stable, while in the anionic state, odd numbered k tends to be more stable.

(2) Since the 6s orbital energy of Au is almost as low as 5d orbitals due to the relativistic effect, the strong s−d hybridization in Au allows gold clusters to be in favor of 1-D and 2-D conformations. This explains the ductility of Au clusters. In contrast, the silver clusters are in favor of 3-D conformation by spherical coordination due to s-type valence orbitals. By the same reason, the average coordination number of an Au atom is small, while that of an Ag atom is large. Au atoms which favor smaller coordination numbers tend to be on the surface/edges/vertices, while Ag atoms which favor higher coordination numbers are inside. In the anionic system, this trend is much stronger. Overall, gold favors 2-D structures, while silver favors 3-D structures from $k = 7$ up to $k = 13$. In the anion systems, the lower dimensional preference is strengthened, and so the 2-D preference is much more pronounced in both gold and silver clusters, and even the 1-D preference can be noted for very small anionic gold clusters. In the alloy, the structures are strongly correlated to the pure gold or silver structures, depending on the ratio of the number of Au atoms to Ag atoms in the cluster.

(3) Since the Ag-5s orbital is much higher in energy than the Au-6s orbital energy, the partial charge transfer from Au to Ag takes place. Thus, Au atoms tend to be negatively charged, while Ag atoms tend to be positively charged. Combined with the trend that Au atoms tend to be near the surface/edges/vertices and Ag atoms tend to be inside (unless the large number of coordination more than 5 is nonspherical or is forced to be on a plane), the outer part of the cluster tends to be negatively charged, and the inner part tends to be positively charged.

(4) The partial charge transfer from Au atoms to Ag atoms provides significant electrostatic stabilization, which makes the alloy formation more favorable than pure gold and silver clusters. The equivalent mixing between Au and Ag atoms in the alloy formation tends to be more favored.

We believe that our work will stimulate further investigation on the mechanism of alloy formation in binary alloys as well as the ductility in making 1-D nanowires and 2-D thin films in other interesting systems,[4] which would open a new branch in chemistry.

Acknowledgment. We are thankful to Prof. V. B. Koutecky for discussions and Prof. A. Nakajima for providing the VDE data prior to publication. The authors are grateful to KISTEP/CRI of the Korean Ministry of Science and Technology for

financial support. The authors would like to thank the Supercomputing Center of Korea Institute of Science and Technology Information.

Note Added in Proof. Several DFT studies of anionic gold clusters[39] and gold−silver clusters[40] have appeared since the submission of the present manuscript (November, 2001). In contrast to those investigations, wherein the focus was on metal clusters, the present study was initiated to elucidate the origin of ductility of gold and the origin of gold−silver alloy formation, to understand the formation of nanostructures involving these metal atoms and organic nanotubes.[9a−d]

References and Notes

(1) (a) Pyykko, P. *Chem. Rev.* **1997**, *97*, 597. (b) Fernandez, E. J.; Gimeno, M. C.; Laguna, A.; Lopez-de-Luzuriaga, J. M.; Monge, M.; Pyykko, P.; Sundholm, D. *J. Am. Chem. Soc*. **2000**, *122*, 7287. (c) Pyykko, P.; Runeberg, N. *Angew. Chem. Ed. Int.* **2002**, *41*, 2174. (d) Pyykko, P.; Zhao, Y. *Angew. Chem. Ed. Int.* **1995**, *34*, 1894.

(2) (a) Schmidt, M.; Kusche, R.; v. Issendorff, B.; Haberland, H. *Nature* **1998**, *393*, 238. (b) Schmidt, M.; Kusche, R.; Hippler, T.; Donges, J.; Kronmuller, W.; v. Issendorff, B.; Haberland, H. *Phys. Rev. Lett.* **2001**, *86*, 1191

(3) (a) Frankamp, B.; Boal, A. K.; Rotello, V. M. *J. Am. Chem. Soc.* **2002**, *124*, 15146. (b) Rawashdeh-Omary, M. A.; Omary, M. A.; Patterson, H. H. *J. Am. Chem. Soc.* **2000**, *122*, 10371. (c) Eberhardt, W. *J. Surf. Sci.* **2002**, *500*, 242.

(4) (a) Geng, W.-T.; Kim, K. S. *Phys. Rev. B* **2003**, *67*, 233403. (b) Nautiyal, T.; Youn, S. J.; Kim, K. S. *Phys. Rev. B* **2003**, *68*, 033407. (c) Suh, S. B.; Hong, B. H.; Tarakeshwar, P.; Youn, S. J.; Jeong, S.; Kim, K. S. *Phys. Rev. B* **2003**, *67*, 241402. (d) Kim, K. S. *Bull. Korean Chem. Soc.* **2003**, *24*, 757. (e) Tarakeshwar, P.; Kim, K. S. In *Encyclopedia of Nanoscience and Nanotechnology;* Nalwa, H. S., Ed.; Academic Press: San Diego, 2003; to be printed.

(5) (a) Thomas, O. C.; Zheng, W.; Bowen, K. H., Jr. *J. Chem. Phys.* **2001**, *114*, 5430. (b) Kruger, S.; Stener, M.; Rosch, N. *J. Chem. Phys.* **2000**, *114*, 5207. (c) Cottancin, E.; Lerme, J.; Gaudry, M.; Pellarin, M.; Vialle, J. L.; Broyer, M. *Phys. Rev. B* **2000**, *62*, 5179. (d) Link, S.; Wang, Z. L.; El-Sayed, M. A. *J. Phys. Chem. B* **1999**, *103*, 3529. (e) Rousset, J. L.; Renouprez, A.; Cadrot, A. M. *Phys. Rev. B* **1998**, *58*, 2150. (f) De Cointet, C.; Khatouri, J.; Mostafavi, M.; Belloni, J. *J. Phys. Chem.* **1997**, *101*, 3517.

(6) Zhang, H.; Zelmon, D. E.; Deng, L.; Liu, H.-K.; Teo, B. K. *J. Am. Chem. Soc.* **2001**, *123*, 11300.

(7) (a) Somorjai, G. A. *Introduction to Surface Chemistry and Catalysis*; John Wiley & Sons: New York, 1994. (b) Rainer, D. R.; Xu, C.; Holmblad, P. M.; Goodman, D. W. *J. Vac. Sci. Technol. A* **1997**, *15*, 1653. (c) Baddeley, C. J.; Tikhov, M.; Hardacre, C.; Lomas, J. R.; Lambert, R. M. *J. Phys. Chem.* **1996**, *100*, 2189. (d) Reifsnyder, S. N.; Lamb, H. H. *J. Phys. Chem. B* **1999**, *103*, 321. (e) Rousset, J. L.; Aires, J. C. S.; Sekhar, R.; Mélinon, P.; Prevel, B.; Pellarin, M. *J. Phys. Chem. B* **2000**, *104*, 543.

(8) (a) Lopez, N.; Norskov, J. K. *J. Am. Chem. Soc.* **2002**, *124*, 11262. (b) Sanchez, A.; Abbet, S.; Heiz, U.; Schneider, W. D.; Hakkinen, H.; Barnett, R. N.; Landman, U. *J. Phys. Chem. A* **1999**, *103*, 9573. (c) Eachus, R. S.; Marchetti, A. P.; Muenter, A. A. *Annu. Rev. Phys. Chem.* **1999**, *50*, 117. (d) Haruta, M. *Catal. Today* **1997**, *36*, 153. (e) Hayat, M. A. *Colloidal Gold: Principles, Methods, and Applications*; Academic Press: San Diego, CA, 1991. (f) Elder, R. C.; Ludwig, Cooper, J. N.; Eidsness, M. K. *J. Am. Chem. Soc.* **1985**, *107*, 5024. (g) Teo, B. K.; Keating, K. *J. Am. Chem. Soc.* **1984**, *106*, 2224.

(9) (a) Hong, B. H.; Bae, S. C.; Lee, C. W.; Jeong, S.; Kim, K. S. *Science* **2001**, *294*, 348. (b) Hong, B. H.; Lee, J. Y.; Lee, C. W.; Kim, J. C.; Bae, S. C.; Kim, K. S. *J. Am. Chem. Soc.* **2001**, *123*, 10748. (c) Kim, K. S. *Curr. Appl. Phys.* **2002**, *2*, 65. (d) Kim, K. S.; Suh, S. B.; Kim, J. C.; Hong, B. H.; Lee, E. C.; Yun, S.; Tarakeshwar, P.; Lee, J. Y.; Kim, Y.; Ihm, H.; Kim, H. G.; Lee, J. W.; Kim, J. K.; Lee, H. M.; Kim, D.; Cui, C.; Youn, S. J.; Chung, H. Y.; Choi, H. S.; Lee, C.-W.; Cho, S. J.; Jeong, S.; Cho, J.-H. *J. Am. Chem. Soc.* **2002**, *124*, 14268. (e) Andres, R. P.; Bein, T.; Dorogi, M.; Feng, S.; Henderson, J. I.; Kubiak, C. P.; Mahoney, W.; Osifchin, R. G.; Reifenberger, R. *Science* **1996**, *272*, 1323. (f) Mirkin, C. A.; Letsinger, R. L.; Mucic, R. C.; Storhoff, J. J. *Nature* **1996**, *382*, 607. (g) Alivisatos, A. P.; Johnson, K. P.; Peng, X.; Wilson, T. E.; Loweth, C. J.; Bruchez, M. P., Jr.; Schultz, P. G. *Nature* **1996**, *382*, 609.

(10) (a)Wilcoxon, J. P.; Martin, J. E.; Parsapour, F.; Wiedenman, B.; Kelley, D. F. *J. Chem. Phys.* **1998**, *108*, 9137. (b) Fedrigo, S.; Harbich, W.; Buttet, J. *J. Chem. Phys*. **1993**, *99*, 5712. (c) Handschuh, H.; Gantefor, G.; Bechthold, P. S.; Eberhardt, W. *J. Chem. Phys.* **1994**, *100*, 7093. (d) Collings, B. A.; Athanassenas, K.; Lacombe, D.; Rayner, D. M.; Hackett, P. A. *J. Chem. Phys*. **1994**, *101*, 3506. (e) Harbich, W.; Fedrigo, S.; Buttet, J.; Lindsay, D. M. *J. Chem. Phys*. **1992**, *96*, 8104. (f) Doremus, R. H. *Langmuir* **2002**, *18*, 2436.

(11) (a) Jackschath, C.; Rabin, I.; Schulze, S. W. *Z. Phys. D* **1992**, *22*, 517; *Ber. Bunsen-Ges. Phys. Chem*. **1992**, *86*, 1200. (b) Alameddin, G.; Hunter, J.; Gameron, D.; Kappes, M. M. *Chem. Phys. Lett*. **1992**, *192*, 122.

(12) (a) Beutel, V.; Kramer, H. G.; Bhale, G. L.; Kuhn, M.; Weyers, L.; Demtroder, W. *J. Chem. Phys*. **1993**, *98*, 2699. (b) Ho, J.; Ervin, K. M.; Lineberger, W. C. *J. Chem. Phys*. **1990**, *93*, 6987. (c) Gantefor, G.; Gausa, M.; Meiwes-Broer, K. H.; Lutz, H. O. *J. Chem. Soc., Faraday Trans.* **1990**, *86*, 2483. (d) Taylor, K. J.; Pettiette-Hall, C. L.; Cheshnovsky, O.; Smally, R. E. *J. Chem. Phys.* **1992**, *96*, 3319. (e) Hotop, H.; Lineberger, W. C. *J. Phys. Chem. Ref. Data* **1985**, *14*, 731.

(13) (a) Ackerman, M.; Stafford, F. E.; Drowart, J. *J. Chem. Phys*. **1960**, *33*, 1784. (b) Bishea, G. A.; Morse, M. D. *J. Chem. Phys.* **1991**, *95*, 5646. (c) Pinegar, J. C.; Langenberg, J. D.; Morse, M. D. *Chem. Phys. Lett.* **1993**, *212*, 458. (d) Hotop, H.; Lineberger, W. C. *J. Phys. Chem. Ref. Data* **1975**, *4*, 539.

(14) Negishi, Y.; Nakamura, Y.; Nakajima, A. *J. Chem. Phys.* **2001**, *115*, 3657.

(15) (a) Hubner, K. P.; Herzberg, G. *Constants of Diatomic Molecules*; Van Norstrand Reinhold: New York, 1979. (b) Fabbi, J. C.; Langenberg, J. D.; Costello, Q. D.; Morse, M. D.; Karlsson, L. *J. Chem. Phys*. **2001**, *115*, 7543. (c) Simard, B.; Hackett, P. A.; James, A. M.; Langridge Smith, P. R. R. *Chem. Phys. Lett.* **1991**, *186*, 415.

(16) Srdanov, V. I.; Pesic, D. S. *J. Mol. Spectrosc*. **1985**, *90*, 27.

(17) Davidson, E. R.; Fain, S. C., Jr. *J. Vac. Sci. Technol*. **1976**, *13*, 209.

(18) (a)Yoon, J.; Kim, K. S.; Baeck, K. K. *J. Chem. Phys.* **2000**, *112*, 9335. (b) Kim, S. H.; Medciros-Ribeiro, G.; Ohlberg, D. A. A.; Williams, R. S.; Heath, J. R. *J. Phys. Chem. B* **1999**, *103*, 10341. (c) Ekardt, W. *Metal Clusters*; Wiley: Chichester, 1999. (d) Garzon, I. L.; Michaelian, K.; Beltran, M. R.; Amarillas, A. P.; Ordejon, P.; Artacho, E.; Portal, D. S.; Soler, J. M. *Phys. Rev. Lett.* **1998**, *81*, 1600. (e) Michaelian, K.; Rendon, N.; Garzon, J. L. *Phys. Rev. B* **1999**, *60*, 2000. (f) Whetten, R. L.; Khoury, J. T.; Alvarez, M. M.; Murthy, S.; Vezmar, I.; Wang, Z. L.; Stephens, P. W.; Cleveland, C. L.; Luedtke, W. D.; Landman, U. *Adv. Mater.* **1996**, *5*, 8. (g) Walch, S. P. *J. Chem. Phys*. **1986**, *85*, 5900.

(19) Wesendrup, R.; Hunt, T.; Schwerdtfeger, P. *J. Chem. Phys*. **2000**, *112*, 9356.

(20) (a) Koutecky, V. B.; Cespiva, L.; Fantucci, P.; Koutecky, J. *J. Chem. Phys*. **1993**, *98*, 7981. (b) Koutecky, V. B.; Cespiva, L.; Fantucci, P.; Pittner, J.; Koutecky, J. *J. Chem. Phys*. **1994**, *100*, 490.

(21) (a) Fournier, R. *J. Chem. Phys*. **2001**, *115*, 2165. (b) Bosnick, K. A.; Haslett, T. L.; Fedrigo, H. S.; Moskovits, M. Chan, W.-T.; Fournier, R. *J. Chem. Phys*. **1999**, *111*, 8867.

(22) Gronbeck, H.; Andreoni, W. *Chem. Phys.* **2000**, *262*, 1.

(23) Hakkinen, H.; Landman, U. *Phys. Rev. B* **2000**, *62*, R2287.

(24) (a) Suzumura, T.; Nakajima, T.; Hirao, K. *Int. J. Quantum Chem*. **1999**, *75*, 757. (b) Bonacic-Koutecky, V.; Veyret, V.; Mitric, R. *J. Chem. Phys*. **2001**, *115*, 10450.

(25) (a) Bauschlicher, C. W., Jr.; Langhoff, S. R.; Partridge, H. *J. Chem. Phys*. **1989**, *91*, 2412. (b) Partridge, H.; Bauschlicher, C. W., Jr.; Langhoff, S. R. *Chem. Phys. Lett*. **1990**, *175*, 531.

(26) (a) Becke, D. *Phys. Rev. A* **1988**, *38*, 3098. (b) Perdew, J. P.; Chevary, J. A.; Vosko, S. H.; Jackson, K. A.; Pederson, M. R.; Singh, D. J.; Fiolhais, C. *Phys. Rev. B* **1992**, *46*, 6671. (c) Perdew, J. P.; Burke, K.; Wang, Y. *Phys. Rev. B* **1996**, *54*, 16533.

(27) Hurley, M. M.; Pacios, L. F.; Christiansen, P. A.; Ross, R. B.; Ermler, W. C. *J. Chem. Phys*. **1986**, *84*, 6840.

(28) Ross, R. B.; Ermler, W. C.; Christiansen, P. A. *J. Chem. Phys*. **1990**, *93*, 6654.

(29) Andrae, D.; Haeussermann, U.; Dolg, M.; Stoll, H.; Preuss, H. *Theor. Chim. Acta* **1990**, *77*, 123.

(30) Martin, J. M. L.; Sundermann, A. *J. Chem. Phys*. **2001**, *114*, 3408.

(31) (a) Frisch, M. J.; Trucks, G. W.; Schlegel, H. B.; Scuseria, G. E.; Robb, M. A.; Cheeseman, J. R.;. Zakrzewski, V. G.; Montgomery, J. A., Jr.; Stratmann, R. E.; Burant, J. C.; Dapprich, S.; Millam, J. M.; Daniels, A. D.; Kudin, K. N.; Strain, M. C.; Farkas, O.; Tomasi, J.; Barone, V.; Cossi, M.; Cammi, R.; Mennucci, B.; Pomelli, C.; Adamo, C.; Clifford, S.; Ochterski, J.; Petersson, G. A.; Ayala, P. Y.; Cui, Q.; Morokuma, K.; Malick, D. K.; Rabuck, A. D.; Raghavachari, K.; Foresman, J. B.; Cioslowski, J.; Ortiz, J. V.; Baboul, A. G.; Stefanov, B. B.; Liu, G.; Liashenko, A.; Piskorz, P.; Komaromi, I.; Gomperts, R.; Martin, R. L.; Fox, D. J.; Keith, T.; Al-Laham, M. A.; Peng, C. Y.; Nanayakkara, A.; Gonzalez, C.; Challacombe, M.; Gill, P. M. W.; Johnson, B. G.; Chen, W.; Wong, M. W.; Andres, J. L.; Head-Gordon, M.; Replogle, E. S.; Pople, J. A. *Gaussian 98*; Gaussian, Inc.: Pittsburgh, PA, 1998. (b) Stanton, J. F.; Gauss, J.; Watts, J. D.; Nooijen, M.; Oliphant, N.; Perera, S. A.; Szalay, P. G.; Lauderdale, W. J.; Kucharski, S. A.; Gwaltney, S. R.; Beck, S.; Balková, A.; Bernholdt, D. E.; Baeck, K. K.; Rozyczko, P.; Sekino, H.; Hober, C.; Bartlett, R. J. *ACES II*, Quantum Theory Project, Florida. The program also contains the integral packages VMOL (Almlöf, J.; Taylor, P. R.); VPROPS (Taylor, P.), and ABACUS (Helgaker, T.; Jensen, H. J. A.; Jørgensen, P.; Olsen, J.; Taylor, P. R.).

(32) Lee, S. J.; Kim, K. S. POSMOL (Reg. No. 2000-01-12-4239), Postech Licensing Center, Pohang, Korea, 2000 (Anonymous ftp address: ftp://csm50.postech.ac.kr/posmol).

(33) (a) Saue, T.; Faegri, K.; Helgaker, T.; Gropen, O. *Mol. Phys.* **1997**, *91*, 937. (b) Suzumura, T.; Nakajima, T.; Hirao, K. *Int. J. Quantum Chem*. **1999**, *75*, 757. (c) Wesendrup, R.; Laerdahl, J. K.; Schwerdtfeger, P. *J. Chem. Phys*. **1999**, *110*, 9457. (d) Motegi, K.; Nakajima, T.; Hirao, K. *J. Chem. Phys*. **2001**, *114*, 6000. (e) Neogrady, P.; Kello, V.; Urban, M.; Sadlej, A. J. *Int. J. Quantum Chem*. **1997**, *63*, 557. (f) Ross, R. B.; Ermler, W. C. *J. Phys. Chem*. **1985**, *89*, 5202. (g) Arratia-Perez, R.; Malli, G. L. *J. Chem. Phys*. **1986**, *84*, 5891.

(34) (a) Leisner, T.; Vajda, S.; Wolf, S.; Woste, L. *J. Chem. Phys.* **1999**, *111*, 1017. (b) Boo, D. W.; Ozaki, Y.; Andersen, L. H.; Lineberger, W. C. *J. Phys. Chem. A* **1997**, *101*, 6688.

(35) (a) Kim, J.; Kim, K. S. *J Chem. Phys*. **1998**, *100*, 5886. (b) Lee, H. M.; Suh, S. B.; Lee, J. Y.; Tarakeshwar, P.; Kim, K. S. *J Chem. Phys*. **2000**, *112*, 9759. (c) Laasonen, K.; Parrinello, M.; Car, R.; Lee, C.; Vanderbilt, D. *Chem. Phys. Lett*. **1993**, *207*, 208.

(36) (a) Legoas, S. B.; Galvao, D. S.; Rodrigues, V.; Ugrate, D. *Phys. Rev. Lett*. **2002**, *88*, 076105. (b) Rubio-Bollinger, G.; Bahn, S. R.; Agrait, N.; Jacobsen, K. W.; Vieira, S. *Phys. Rev. Lett.* **2001**, *87*, 026101. (c) Rodrigues, V.; Ugarte, D. *Nanotechnology* **2002**, *13*, 404. (d) Mozes, J. L.; Ordejon, P.; Brandbyge, M.; Taylor, J.; Stokbro, K. *Nanotechnology* **2002**, *13*, 346. (e) Todorov, T. N.; Hoekstra, J.; Sutton, A. P. *Phys. Rev. Lett*. **2001**, *86*, 3606. (f) Rodrigues, V.; Ugrate, D. *Phys. Rev. B* **2001**, *63*, 073405. (g) Sanchez-Portal, D.; Artacho, E.; Junquera, J.; Ordejon, P.; Garcia, A.; Soler, J. M. *Phys. Rev. Lett*. **1999**, *83*, 2884. (h) Yanson, A. I.; Rubio-Bollinger, G.; van den Brom, H. E.; Agrait, N.; van Ruitenbeek, J. M. *Nature* **1998**, *395*, 783. (i) Landman, U.; Luedtke, W. D.; Salisbury, B. E.; Whetten, R. L. *Phys. Rev. Lett*. **1996**, *77*, 1362.

(37) (a) Majumdar, D.; Kim, J.; Kim, K. S. *J. Chem. Phys*. **2000**, *112*, 101. (b) Kim, J.; Lee, H. M.; Suh, S. B.; Majumdar, D.; Kim, K. S. *J. Chem. Phys*. **2000**, *113*, 5259. (c) Lee, H. M.; Kim, K. S. *J. Chem. Phys*. **2001**, *114*, 4461. (d) Kim, K. S.; Suh, S. B.; Kim, J. C.; Hong, B. H.; Lee, E. C.; Yun, S.; Tarakeshwar, P.; Lee, J. Y.; Kim, Y.; Ihm, H.; Kim, H. G.; Lee, J. W.; Kim, J. K.; Lee, H. M.; Kim, D.; Cui, C.; Youn, S. J.; Chung, H. Y.; Choi, H. S.; Lee, C.-W.; Cho, S. J.; Jeong, S.; Cho, J.-H. *J. Am. Chem. Soc*. **2002**, *124*, 14268. (e) Lee, S. J.; Cho, S. J.; Oh, K. S.; Cui, C.; Ryu, Y.; Chang, Y.-T.; Kim, K. S.; Chung, S.-K. *J. Phys. Chem*. **1996**, *100*, 10111. (f) Kim, K. S.; Tarakeshwar, P.; Lee, J. Y. *Chem. Rev*. **2000**, *100*, 4145.

(38) (a) Suh, S. B.; Lee, H. M.; Kim, J.; Lee, J. Y.; Kim, K. S. *J. Chem. Phys*. **2000**, *113*, 5273. (b) Lee, S.; Kim, J.; Lee, S. J.; Kim, K. S. *Phys. Rev. Lett.* **1997**, *79*, 2038.

(39) (a) Hakkinen, H.; Moseler, M.; Landman, U. *Phys. Rev. Lett*. **2002**, *89*, 033401. (b) Furche, F.; Ahlrichs, R.; Weis, P.; Jacob, C.; Gilb, S.; Bierweiler, T.; Kappes, M. M. *J. Chem. Phys*. **2002**, *117*, 6982. (d) Wang, J.; Wang, G.; Zhao, *J. Phys. Rev. B* **2002**, *66*, 035418. (e) Oviedo, J.; Palmer, R. E. *J. Chem. Phys*. **2002**, *117*, 9548.

(40) Bonacic-Koutecky, V.; Burda, J.; Mitric, R.; Ge, M.; Zampella, G.; Fantucci, P. *J. Chem. Phys*. **2002**, *117*, 3120.